Published in final edited form as:

Urol Res. 2012 October ; 40(5): 447–454. doi:10.1007/s00240-012-0459-1.

Relative deficiency of acidic isoforms of osteopontin from stone former urine

A. M. Kolbach,

Nephrology Division, Department of Medicine, Medical College of Wisconsin and the Department of Veterans Affairs Medical Center, 5000 W National Avenue, Milwaukee, WI 53295, USA

O. Afzal,

Nephrology Division, Department of Medicine, Medical College of Wisconsin and the Department of Veterans Affairs Medical Center, 5000 W National Avenue, Milwaukee, WI 53295, USA

B. Halligan,

Biotechnology and Bioengineering Center, Medical College of Wisconsin, 8701 Watertown Plank Road, Milwaukee, WI 53226, USA

E. Sorokina,

Nephrology Division, Department of Medicine, Medical College of Wisconsin and the Department of Veterans Affairs Medical Center, 5000 W National Avenue, Milwaukee, WI 53295, USA

J. G. Kleinman, and

Nephrology Division, Department of Medicine, Medical College of Wisconsin and the Department of Veterans Affairs Medical Center, 5000 W National Avenue, Milwaukee, WI 53295, USA

J. A. Wesson

Nephrology Division, Department of Medicine, Medical College of Wisconsin and the Department of Veterans Affairs Medical Center, 5000 W National Avenue, Milwaukee, WI 53295, USA

J. G. Kleinman: kleinman@mcw.edu

Abstract

We have tested the relative electrophoretic mobility of osteopontin (OPN) isolated from urine obtained from normal individuals (NU) against similar samples derived from the urine of stone formers (SFU) using high-resolution isoelectric focusing (isoelectric point, pI range 3.5–4.5) in 2D electrophoresis, with Western blot detection. We also report the results from competitive ELISA analyses of these samples. We demonstrated that human urinary OPN has a discrete four band separation pattern that conforms to four previously documented OPN isoforms. The lower two M_r isoforms migrate to a greater degree toward the acidic end of the gel than do the higher two M_r isoforms. Densitometry of the signal reveals significant difference in the migration pattern of OPN from SFU as compared to that from NU based on an analysis of the spot intensities grouped in 0.1 pI unit increments. A novel method for the calculation of a weight-averaged pI based on the relative signal strength in an OPN 2D Western blot was developed. The analysis revealed a significantly increased weight-averaged pI values for the higher M_r forms of OPN in the stone former compared to normal population. Additionally, alkaline phosphatase-treated NU samples

Correspondence to: J. G. Kleinman, kleinman@mcw.edu.

resulted in a significant average pI shift of 0.05 units in the alkaline direction, suggesting that a decrease in the average degree of phosphorylation could be responsible for the difference between NU and SFU pI.

Keywords

Nephrolithiasis; Osteopontin; Electrophoretic mobility; Isoelectric point

Introduction

Normal human urine prevents calcium oxalate crystallization, and urinary macromolecules are thought to account for most of this inhibitory property [1]. One characteristic that inhibitory macromolecules for stone formation appear to share is that they are relatively anionic. This property can be attributed to the combination of anionic amino acids in a protein backbone and the presence of various post-translational modifications, such as sialylation, sulfation, or phosphorylation. The pathogenesis of calcium oxalate stone formation may depend on either reduced amounts of these macromolecular inhibitors or defects in their ionic structure.

One such macromolecule, osteopontin (OPN), inhibits attachment of calcium oxalate crystals to renal epithelial cells and also crystal nucleation, growth, and aggregation in vitro [2–4]. Additionally, OPN null mice are more susceptible to renal crystal deposition [5, 6]. OPN undergoes significant post-translational modification, and several studies have identified as many as 29–33 putative phosphorylation and 6–7 glycosylation sites by mass spectroscopic analysis [7, 8]. There is evidence that phosphorylation may play a role in its inhibitory effects on crystal formation [9–11]. The aim of this study was to detect any difference between the anionic characteristics of the OPN in stone former urine (SFU) and normal urine (NU) by examining both their relative quantity and isoelectric point (pI). We hypothesized that OPN from stone formers will demonstrate reduced phosphorylation, glycosylation, or both, corresponding to impaired macromolecular inhibitor function. These changes would be observable as an increase in the average isoelectric point in 2D gel electrophoresis (alkaline shift), corresponding to the reduction in negatively charged side chains.

In the experiments described below, we have tested the relative mobilities of NU and SFU OPN in high-resolution isoelectric focusing (IEF) (pI range 3.5–4.5) 2D electrophoresis experiments with Western blotting detection. One-dimensional PAGE Western blot analysis was performed to assess the relative abundance of the OPN isoforms. We also report the urinary concentrations of OPN by competitive ELISA analysis of the samples.

Materials and methods

Urine collection

Fresh random urine specimens were collected from normal individuals and stone former patients with an EDTA-free protease inhibitor tablet (Roche Applied Science, India-napolis, IN). Normal urine (NU) was obtained from individuals without a personal or familial history

of stones. SFU was obtained from patients with recurrent calcium oxalate stones from the Stone Clinic at the Froedtert Memorial Lutheran Hospital in Milwaukee and the Nephrology Clinic the Milwaukee Veterans Affairs Medical Center. Both groups had normal renal function, and were negative for protein by urine dipstick, and were of comparable ages. Individuals on medications that could affect renal function (NSAIDS, ACEI, ARB), diabetics, hypercalciurics (Ca/creatinine > 300 mg/g), and individuals with proteinuria (protein/creatinine > 200 mg/g) were excluded from this study. These exclusions were utilized to eliminate the confounding effects of large numbers of abnormal proteins in the urine and to increase our chances of finding a hitherto unrecognized urinary abnormality, such as a difference in urinary proteins, in stone forming subjects. Urinary calcium, creatinine, and protein analyses were performed by the clinical chemistry laboratory (VA Medical Center, Milwaukee, WI). The Institutional Review Board and the Research Committee of the respective institutions approved the studies.

Urine macromolecule preparation

Urine macromolecules were isolated by ultradiafiltration (10 kD MiniKros, Spectrum Laboratories, CA) against a buffer containing 100 mM NaCl. The macromolecular fractions were concentrated five- to tenfold during this process, and were constantly in the presence of protease inhibitors (Sigma) from the time of collection. Samples were stored at −80°C until assayed. Equivalent amounts urine protein were assayed in a Western blot, as described below, before and after ultrafiltration to ensure no appreciable losses or degradation in osteopontin occurred. Protein measurements were made using a coomassie blue based colorimetric assay (Protein Dye Reagent, Biorad, Hercules, CA) using a bovine serum albumin as a standard.

Osteopontin assay

Ultradiafiltered samples were analyzed for total OPN concentrations using a competitive ELISA. GST-human OPN (cDNA construct a kind gift of Novartis AG, Emeryville, CA op-30 [Nucleic Acids Research, 17(8)3308, 1989)] was used as a standard and to coat (0.2 μg/ml in PBS) 96-well plates. Samples were added to a blocked plate (0.25% gelatin-PBS) in a serial dilution manner competing with polyclonal anti-human OPN antibodies (LF123, rabbit, a gift from Larry Fisher, National Institutes of Health) [12]. Secondary antibody and streptavidin complex was provided for in Vector ABC kit (Vector Laboratories, Burlingame, CA-PK 4001). *O*-phenylenediamine was used as a substrate, stopping the reaction with 4% H_2SO_4.

1D gel electrophoresis and osteopontin Western detection

Samples of urine macromolecules were separated on a 4–12% Bis, Tris polyacrylamide gel system using MOPS buffer (Invitrogen, Grand Island, NY), blotted to 0.2 μm nitrocellulose and probed for human OPN using a polyclonal antibody made in our lab against GST-hOPN. Chemiluminescence was performed (SuperSignal West Femto, Thermo Scientific, Rockford, IL) and recorded by exposure to X-ray films. M_r estimations were made using See Blue MWS (Invitrogen, Grand Island, NY) or Biorad low range standards (Hercules, CA).

2D gel electrophoresis and osteopontin Western detection

2D gel analysis or IEF was performed by focusing 10 μg urinary macromolecule samples on an immobilized gradient 18 cm strips (Immobiline IEF 3.5–4.5 pH, GE Healthcare Life Sciences, Piscataway, NJ). The strips were soaked overnight with protease and phosphatase inhibitors and focused at 3,000 V for 12 h. The second dimension of the most acidic region of the IEF strip, the first 11 cm or 3.5–4.2 pI, was separated on a Criterion 4–12% Bis Tris polyacrylamide gel system using MOPS buffer (Biorad, Hercules, CA), blotted and probed as described for 1D gels. The immobilized IEF strips were calibrated using IEF standards (Serva, Heidelberg, Germany). The calibration standards used on these narrow range IEF strips revealed the 3.5 and 4.5 pI standards migrating at the very ends of the strips. A linear relationship between pI and gel position was assumed to interpolate the remaining pI mobility estimates. The intense signal at pI = 3.5 suggested that there may have been some stacking of OPN isoforms with pI values <3.5 at this extreme position on the gel. While the current gel system was unable to resolve OPN isoforms with pI values 3.5 or less, no other immobilized gradient tested in our lab gave the clarity or resolution demonstrated in these strips. In order to facilitate testing in our lab the IEF strip was cut into two portions, the acidic (the first 11 cm) and the basic end. No signal was detected in the basic portion of the IEF strip (pI 4.2–4.5).

Densitometry

Human urinary OPN migrates on standard gel electrophoresis in four characteristic bands (Fig. 1). The first and third bands often predominate, while the second and fourth bands appear to be in lesser abundance. 2D Western blot analysis of the same samples (Fig. 2) reveals that the higher M_r bands (1 and 2) follow more similar pI distribution patterns, while the lower M_r bands (3 and 4) appear to co-migrate. These patterns of co-migration along with slight shifts in molecular weight with varied isoelectric point suggest that stronger analysis could be obtained by considering the higher M_r and lower M_r bands as pairs, rather than individually, when conducting the extensive densitometric analysis.

The relative abundance of the higher M_r OPN isoforms (OPN 1 and 2) as compared to the lower M_r OPN isoforms (OPN 3 and 4) was measured by comparing pixel intensity on photo-documented X-ray films (MI software, Care-stream Health, Rochester, NY). The relative abundance of OPN total and the higher and the lower M_r OPN isoforms were quantified using gel analysis software developed at the Medical College of Wisconsin Biotechnology and Bioengineering Center. Briefly, this involves dividing the blot into 0.1 pI unit segments and measuring the pixel intensity as a percentage of the entire signal measured. Additionally, the gel analysis software generated a weight-averaged isoelectric point for all OPN bands and for OPN 1 and 2, and OPN 3 and 4 bands.

Osteopontin dephosphorylation

Ultradiafiltered urine macromolecule samples were enzymatically dephosphorylated using alkaline phosphatase (2 h at 37°C, in CAIP buffer, GE Healthcare Life Sciences, Piscataway, NY). Enzyme free samples were also incubated at 37°C in buffer as a control. The prepared samples were focused on IEF strips and 2D analysis was performed as described above.

Data analysis

All measured values are expressed as M ± SD (M = mean, SD = standard deviation), except the 0.1 pI incremental analysis (Fig. 3a–c) where SE (SE = standard error) bars are shown. Differences between sample populations were determined using Student's *t* test with $P < 0.05$ defining significance using two-tailed distributions with homoscedastic variance, unless otherwise noted.

Results

The patient urine macromolecules tested in this study were a subset of the samples previously analyzed for their effect on calcium oxalate crystal aggregation [13]. The patients selected were not significantly different in age between stone formers and normals or from the larger groups in the earlier study (Table 1). Efforts were made to collect patients with normal calcium and protein excretion rates based on medical history. The resultant random, non-fasting urine samples from the stone formers contained significantly higher calcium and protein concentrations than those from normals, despite the fact that they fell within the normal range of these parameters and met the inclusion criteria set at the start of the study. An entire urine chemistry panel was not collected for this study, but a urine dipstick was performed. The dipstick specific gravity indicated that the SFUs were less concentrated than those of the normals ($P = 0.04$). There was no significant difference in measured pH. A review of participant medical history showed that the normal panel contained one individual on medications for both hypertension and elevated lipids. The stone former population contained four individuals that were treated for hypertension, two of these four were on citrate therapy, and one of these four was also on medication for elevated lipids.

OPN 1D Western blotting

Migration of human urinary OPN yields four bands (OPN 1–4) as shown in Fig. 1. The relative mobility yielded molecular weight estimates of 56, 51, 48, and 45 kDa using Novex standards or 67, 61, 59, and 54 kDa with Biorad standards. OPN has an estimated amino acid backbone between 32 and 35 kDa, but due to post-translational modifications (i.e., glycosylation and phosphorylation) it is generally accepted that OPN migrates at a much higher molecular weight [14]. The predicted molecular weights obtained using the Novex standards were closer to the expected values and have been used throughout the remainder of this study. The relative abundance of the OPN 1 and 2 was compared to OPN 3 and 4 for the NU and SFU populations tested. OPN 1 and 2 aggregated signals accounted for 72 ± 10% of the signal in the NU population and 67 ± 10% of the signal in the SFU tested. The difference did not reach statistical significance.

OPN ELISA analysis

Urinary OPN values have been reported in the range of 3–5 μg/ml using ELISA methods [15]. Analysis of the NU and SFU panels yielded average urinary concentrations of 4 and 2.6 μg/ml, respectively (Table 2). When normalized for urinary creatinine concentrations, these values were 2.5 and 3 μg/mg creatinine for the NU and SFU panels, respectively. Independent of whether the OPN concentrations were expressed in absolute or normalized concentration units, there was no statistical difference between OPN concentrations in the

NU and SFU panels. The trend toward lower absolute concentrations of OPN in the face of the opposite trend in normalized concentrations in SFU samples may have resulted from efforts by these patients to drink more fluid to prevent stone recurrence. While some have suggested that OPN promotes stone disease (vide infra) and have demonstrated in vitro that OPN is secreted in response to crystal formation, the OPN concentrations normalized for creatinine concentration were not statistically different between the NU and SFU panels [16–19].

2D OPN Western blots

High-resolution 2D PAGE of OPN (Fig. 2) consistently shows signal between pI values of 3.5–4.1. Generally, OPN 1 and 2 bands separated into a series of spots that were more basic (pI ranges from 3.6 to 4.1), while OPN 3 and 4 bands separated into a series of spots that were more acidic (pI ranges from 3.5 to 3.8). The decrease in signal in the 3.5–3.7 pI range for the SFU OPN 1 and 2 (highlighted in Fig. 2 by large ovals) was reflected in the significant increase in the calculated weight-averaged isoelectric point for these isoforms (Table 3). The increase in signal in the 3.7–3.8 pI range for OPN 3 and 4 (highlighted with the small ovals) did not significantly affect the overall weight-averaged pI for these isoforms. Due to limited amounts of material, the samples were generally run only once. The reproducibility of the method is shown from the analysis of duplicate samples which resulted in weight-averaged pI determinations of 3.811 ± 0.004, 3.83 ± 0.024, and 3.77 ± 0.03 for all OPN bands, OPN bands 1 and 2, and OPN bands 3 and 4, respectively.

Densitometric analysis of the 2D Western blot at 0.1 pI increments was used to examine the relative protein distribution patterns (Fig. 3a–c). The bars represent the total pixel density within any given pI range for the OPN region of interest (i.e., the range of 3.50–3.59 is represented by the bars at 3.5). The OPN total signal (Fig. 3a) analysis revealed a significant decrease in the 3.6 isoelectric point region for SFU compared to NU ($P = 0.04$; two-tailed, paired). The OPN 1 and 2 regional analyses (Fig. 3b) showed a significant decrease in both the 3.5 and 3.6 signals in SFU as compared to NU ($P = 0.02$ and 0.05, respectively). Conversely, the OPN 3 and 4 regional analysis (Fig. 3c) showed a significant increase in the midrange 3.7 signal in SFU as compared to NU ($P = 0.05$). Overall, SFU OPN samples showed a significant decrease in the most acidic pI ranges (3.5 and 3.6) and a significant increase in the midrange pI range (3.7).

These observations were reinforced by the weight-averaged pI analysis calculated with the gel analysis program (Table 3). OPN total trended toward an increase in pI as suggested by the near significant shift in the weight-averaged pI analysis. The combined OPN 1 and 2 bands did show a significant increase of weight-averaged pI from 3.77 to 3.81, for NU and SFU, respectively ($P = 0.012$). The combined OPN 3 and 4 bands, however, revealed no significant shifts in weight-averaged pI.

Alkaline phosphatase-treated urine macromolecules showed a shift in weight-averaged pI ranging from 0.03 to 0.05 pI units. Table 4 shows the increased weight-averaged pI for OPN following dephosphorylation.

Discussion and conclusions

We compared urinary OPN concentrations, relative molecular weight distribution of OPN isoforms, and weight-averaged isoelectric points from samples collected from normal and stone forming individuals. Osteopontin concentrations reported either as μg/ml or normalized for creatinine were not statistically different between the two populations tested; the total concentrations observed were consistent with the current literature [15]. We and others have shown that human urinary OPN will migrate in four primary isoforms in standard PAGE gels [20–23]. The higher M_r isoforms (OPN bands 1 and 2) comprise approximately two-thirds of the signal intensity and this fraction was similar in both populations. The high-resolution IEF in 2D PAGE analysis of OPN, however, did reveal a significant difference: the weight-averaged pI values for the two higher M_r isoforms of OPN in SFU were more alkaline, i.e., less negatively charged, than similar M_r bands from NU.

The normal panel was selected to match the stone former population as nearly as possible. The measured specific gravity of the SFU population was lower suggesting patient compliance with instructions to increase fluid intake. There was no overall correlation between the specific gravity or the Ca/Cr and the weight-averaged OPN isoelectric point in either group.

The normal population contained one individual on treatment for both hypertension and elevated lipid. This individual's weight-averaged pI values for OPN fell within the normal ranges as did the overall OPN concentration. The stone former population had four individuals on hydrochlorothiazide, a hypertension treatment also used as a stone therapy. Two of four of these patients were also on citrate therapy. The higher M_r OPN pI values were shifted in the alkaline direction in three of the four samples from individuals taking hydrochlorothiazide.

It has been demonstrated by Nemir et al. [24] that non-phosphorylated OPN from rat kidney cells has a higher isoelectric point (4.5) using 2D PAGE as compared to phosphorylated OPN (3.8). Their study, however, was performed on a much broader pI gradient. The 2D analysis in this current study was performed on the acidic end (the first 11 cm) of an 18 cm 3.5–4.5 pI IEF strip. This allowed the characterization of small changes of pI to be noted. All measurements were made digitally by measuring pixels, but it translates to a 0.006 pI change per millimeter measured on the blot. The weight-averaged isoelectric point data (Table 3) suggests an averaged change in pI of 0.04 for the NU versus SFU comparison of OPN 1 and 2. These differences would be equivalent to shifts of ~7 mm on these high-resolution 2D blots, thus, unlikely to be detectable in standard 2D gels.

The Swiss Protein database (http://www.uniprot.org, P10451) describes four isoforms of OPN (a–d) due to various amino acid sequence variations. The molecular weight ranges for the OPN isoforms (a–d) are 35.4, 33.8, 32.4, and 33 kDa with amino acid backbone isoelectric point predictions of 4.37, 4.39, 4.35, and 4.56, respectively. The inclusion of phosphoryl and glycosyl residues to these amino acid backbone structures would easily account for the shifting of pI as a result of IEF analysis of the urine panel presented here.

Attempts by other methodologies to identify the pI shifts that were due exclusively to phosphorylation were limited by the small amounts of available sample. These methods were also not specific to OPN, and assays such as phosphostaining would reflect the phosphorylation state of the entire urine proteome represented in the samples assayed. The goal of the dephosphorylation experiments was to note if shifts in isoelectric point following the removal of some of the phosphate moieties would track similarly to the shifting 2D patterns seen in our study samples. The dephosphorylation experiments do not preclude that these shifts might be due to other charged side groups such as variations in glycosylation, but are given as an example of a post-translational event that might be responsible for the observed sample shifts.

These results are consistent with the in silico prediction of OPN phosphorylation (http://proteomics.mcw.edu/promost.html). Using the Swiss Protein identifier for OPN, P10451, pI values can be calculated for the addition of phosphate moieties. The average shift in pI per phosphate group is 0.030 ± 0.005. The magnitude of the difference in pI between NU and SFU in OPN 1 and 2 in comparison to those observed in enzymatically dephosphorylated OPN from NU suggests that they could be accounted for by decreases in average phosphorylation on the order of 1 or 2 phosphate groups. The change in phosphorylation, however, may not be broadly distributed, rather the more highly phosphorylated molecules may suffer dephosphorylation that is greater than the 1–2 phosphate groups. Even though the weight-averaged values only suggest a 0.05 pI average change in pI (Table 4), the lower pI regions (3.5–3.8) suffered substantial losses, while the higher pI regions (>3.9) appeared to dominate the profile. A similar pattern is observed in the comparison between NU and SFU as shown in Fig. 3b.

The role of OPN in stone disease is controversial. OPN was first identified as an inhibitor of crystal growth [2, 25]. Inhibition of nucleation of both calcium oxalate and hydroxyapatite has also been reported [3, 26]. Moreover, OPN null mice have been reported to accumulate calcium oxalate in their kidneys with ethylene glycol feeding, whereas OPN +/+ mice do not [5]. Another strain of OPN-knockouts has been reported to develop renal hydroxyapatite deposits spontaneously [6]. These studies are consistent with OPN exerting a protective role against stone formation.

On the other hand, there are reports that appear consistent with a stone promotion role for OPN. Some in vitro studies have reported that OPN expression in cultured cells promotes adhesion of calcium oxalate crystals [16, 17]. In addition, OPN has been reported to be present in stone matrix and in the interface between the exposed surfaces of Randall's plaques and the calcium oxalate component of adherent stones [27, 28]. These studies, as well as the numerous reports of localization of OPN in other calcified tissues, have suggested that this molecule may promote adhesion of crystals or other mineralized phases [29].

Studies from our laboratory suggest that a given macromolecule in urine can defend against or actually promote crystal aggregation, a process that we consider crucial for the development of stones, depending on its ability to either self-associate or associate with other macromolecules [13, 30]. Whether a given macromolecule acts as an aggregation

inhibitor or aggregates with other molecules and thereby promotes calcium oxalate aggregation appears to correlate with its net charge or isoelectric point, which, in turn, can be influenced by loss of anionic side chains. This has been demonstrated to be the case for Tamm–Horsfall protein [30].

With respect to OPN, it is evident that in its phosphorylation state OPN is important to its role in crystal growth. Recent studies have shown that OPN inhibits calcium oxalate crystal growth dependent on phosphate content, and that these interactions with the crystal surface are face-specific [31–33]. Its effect to inhibit aggregation is likely to be similarly influenced by phosphorylation, although this has not been directly assessed.

In conclusion, the current studies demonstrate a difference in a physical property of OPN in urine from stone formers, specifically an increase in average isoelectric point. This change is due to a significant decline in the most anionic of the OPN isoforms identified on electrophoresis. A change in the degree of phosphorylation, glycosylation, or both of OPN may be responsible for this change, and a decrease in the net charge of OPN along with other urinary macromolecules could be a factor promoting stone formation. Further studies are needed to uncover the possible mechanisms (e.g., oxidative stress) which might account for the loss of phosphate or other anionic moieties in the stone forming populations. When considered together with studies showing chemical alterations in Tamm–Horsfall protein and its potential for altering physical properties [30, 34], these studies point toward a general mechanism for stone formation that might be amenable to therapeutic interventions.

Acknowledgments

Portions of this work were performed during a period when JAW was supported by a career development award from the Department of Veterans Affairs. Other support was derived from grants to JAW (DK 082250) and JGK (DK 48504) by the NIDDK.

References

1. Khan SR, Kok DJ. Modulators of urinary stone formation. Front Biosci. 2004; 9:1450–1482. [PubMed: 14977559]
2. Worcester EM, Blumenthal SS, Beshensky AM, Lewand DL. The calcium oxalate crystal growth inhibitor protein produced by mouse kidney cortical cells in culture is osteopontin. J Bone Miner Res. 1992; 7:1029–1036. [PubMed: 1414495]
3. Worcester EM, Beshensky AM. Osteopontin inhibits nucleation of calcium oxalate crystals. Ann N Y Acad Sci. 1995; 760:375–377. [PubMed: 7785921]
4. Lieske JC, Leonard R, Toback FG. Adhesion of calcium oxalate monohydrate crystals to renal epithelial cells is inhibited by specific anions. Am J Physiol (Ren Fluid Electrolyte Physiol). 1995; 268(37):F604–F612.
5. Wesson JA, Johnson RJMM, Beshensky AM, Stietz S, Giachelli C, Liaw L, Alpers CE, Couser WG, Kleinman JG, Hughes J. Osteopontin is a critical inhibitor of calcium oxalate crystal formation and retention in renal tubules. J Am Soc Nephrol. 2003; 14:139–147. [PubMed: 12506146]
6. Mo L, Liaw L, Evan AP, Sommer AJ, Lieske JC, Wu XR. Renal calcinosis and stone formation in mice lacking osteopontin, Tamm–Horsfall protein, or both. Am J Physiol Ren Physiol. 2007; 293:F1935–F1943.
7. Sorensen ES, Hojrup P, Petersen TE. Posttranslational modifications of bovine osteopontin: identification of twenty-eight phosphorylation and three *O*-glycosylation sites. Protein Sci. 1995; 4:2040–2049. [PubMed: 8535240]

8. Keykhosravani M, Doherty-Kirby A, Zhang C, Brewer D, Goldberg HA, Hunter GK, Lajoie G. Comprehensive identification of post-translational modifications of rat bone osteopontin by mass spectrometry. Biochemistry. 2005; 44:6990–7003. [PubMed: 15865444]
9. Hoyer JR, Asplin JR, Otvos L Jr. Phosphorylated osteopontin peptides suppress crystallization by inhibiting the growth of calcium oxalate crystals. Kidney Int. 2001; 60:77–82. [PubMed: 11422738]
10. Pampena DA, Robertson KA, Litvinova O, Lajoie G, Goldberg HA, Hunter GK. Inhibition of hydroxyapatite formation by osteopontin phosphopeptides. Biochem J. 2004; 378:1083–1087. [PubMed: 14678013]
11. Razzouk S, Brunn JC, Qin C, Tye CE, Goldberg HA, Butler WT. Osteopontin posttranslational modifications, possibly phosphorylation, are required for in vitro bone resorption but not osteoclast adhesion. Bone. 2002; 30:40–47. [PubMed: 11792563]
12. Fisher LW, Stubbs JT, Young MF. Antisera and cDNA probes to human and certain animal model bone matrix noncollagenous proteins. Acta Orthop Scand Suppl. 1995; 266:61–65. [PubMed: 8553864]
13. Wesson JA, Ganne V, Beshensky AM, Kleinman JG. Regulation by macromolecules of calcium oxalate crystal aggregation in stone formers. Urol Res. 2005; 33:206–212. [PubMed: 15864572]
14. Prince CW, Oosawa T, Butler WT, Tomana M, Bhown AS, Bhown M, Schrohenloher RE. Isolation, characterization, and biosynthesis of a phosphorylated glycoprotein from rat bone. J Biol Chem. 1987; 262:2900–2907. [PubMed: 3469201]
15. Hoyer JR, Pietrzyk RA, Liu H, Whitson PA. Effects of microgravity on urinary osteopontin. J Am Soc Nephrol. 1999; 10(Suppl 14):S389–S393. [PubMed: 10541270]
16. Yamate T, Kohri K, Umekawa T, Amasaki N, Isikawa Y, Kurita T. The effect of osteopontin on the adhesion of calcium oxalate crystals to Madin-Darby canine kidney cells. Eur Urol. 1996; 30:388–393. [PubMed: 8931975]
17. Yamate T, Kohri K, Umekawa T, Iguchi M, Kurita T. Osteopontin antisense oligonucleotide inhibits adhesion of calcium oxalate crystals in Madin-Darby canine kidney cell. J Urol. 1998; 160:1506–1512. [PubMed: 9751404]
18. Kohri K, Nomura S, Kitamura Y, Nagata T, Yoshioka K, Iguchi M, Yamate T, Umekawa T, Suzuki Y, Sinohara H, Kurita T. Structure and expression of the mRNA encoding urinary stone protein (osteopontin). J Biol Chem. 1993; 268:15180–15184. [PubMed: 8325891]
19. Lieske JC, Hammes MS, Hoyer JR, Toback FG. Renal cell osteopontin production is stimulated by calcium oxalate monohydrate crystals. Kidney Int. 1997; 51:679–686. [PubMed: 9067899]
20. Kleinman JG, Wesson JA, Hughes J. Osteopontin and calcium stone formation. Nephron Physiol. 2004; 98:43–47.
21. Denhardt DT, Giachelli CM, Rittling SR. Role of osteopontin in cellular signaling and toxicant injury. Annu Rev Pharmacol Toxicol. 2001; 41:723–749. [PubMed: 11264474]
22. Kazanecki CC, Uzwiak DJ, Denhardt DT. Control of osteopontin signaling and function by post-translational phosphorylation and protein folding. J Cell Biochem. 2007; 102:912–924. [PubMed: 17910028]
23. Kazanecki CC, Kowalski AJ, Ding T, Rittling SR, Denhardt DT. Characterization of anti-osteopontin monoclonal antibodies: binding sensitivity to post-translational modifications. J Cell Biochem. 2007; 102:925–935. [PubMed: 17786932]
24. Nemir M, DeVouge MW, Mukherjee BB. Normal rat kidney cells secrete both phosphorylated and nonphosphorylated forms of osteopontin showing different physiological properties. J Biol Chem. 1989; 264:18202–18208. [PubMed: 2808373]
25. Shiraga H, Min W, VanDusen WJ, Clayman MD, Miner D, Terrell CH, Sherbotie JR, Foreman JW, Przysiecki C, Neilson EG, Hoyer JR. Inhibition of calcium oxalate crystal growth in vitro by uropontin: another member of the aspartic acid-rich protein superfamily. Proc Natl Acad Sci USA. 1992; 89:426–430. [PubMed: 1729712]
26. Boskey AL, Maresca M, Ullrich W, Doty SB, Butler WT, Prince CW. Osteopontin-hydroxyapatite interactions in vitro: inhibition of hydroxyapatite formation and growth in a gelatin-gel. Bone Miner. 1993; 22:147–159. [PubMed: 8251766]

27. de Bruijn WC, de Water R, van Run PR, Boeve ER, Kok DJ, Cao LC, Romijn HC, Verkoelen CF, Schroder FH. Ultrastructural osteopontin localization in papillary stones induced in rats. Eur Urol. 1997; 32:360–367. [PubMed: 9358227]

28. Evan AP, Coe FL, Lingeman JE, Shao Y, Sommer AJ, Bledsoe SB, Anderson JC, Worcester EM. Mechanism of formation of human calcium oxalate renal stones on Randall's plaque. Anat Rec (Hoboken). 2007; 290:1315–1323. [PubMed: 17724713]

29. McKee MD, Nanci A. Osteopontin: an interfacial extra-cellular matrix protein in mineralized tissues. Connect Tissue Res. 1996; 35:251–259.

30. Viswanathan P, Rimer JD, Kolbach AM, Ward MD, Kleinman JG, Wesson JA. Calcium oxalate monohydrate aggregation induced by aggregation of desialylated Tamm–Horsfall protein. Urol Res. 2011; 39:269–282. [PubMed: 21229239]

31. Langdon A, Wignall GR, Rogers K, Sorensen ES, Denstedt J, Grohe B, Goldberg HA, Hunter GK. Kinetics of calcium oxalate crystal growth in the presence of osteopontin isoforms: an analysis by scanning confocal interference microcopy. Calcif Tissue Int. 2009; 84:240–248. [PubMed: 19189038]

32. Chien YC, Masica DL, Gray JJ, Nguyen S, Vali H, McKee MD. Modulation of calcium oxalate dihydrate growth by selective crystal-face binding of phosphorylated osteopontin and polyaspartate peptide showing occlusion by sectoral (compositional) zoning. J Biol Chem. 2009; 284:23491–23501. [PubMed: 19581305]

33. Qiu SR, Wierzbicki A, Orme CA, Cody AM, Hoyer JR, Nancollas GH, Zepeda S, De Yoreo JJ. Molecular modulation of calcium oxalate crystallization by osteopontin and citrate. Proc Natl Acad Sci USA. 2004; 101:1811–1815. [PubMed: 14766970]

34. Sumitra K, Pragasam V, Sakthivel R, Kalaiselvi P, Varalakshmi P. Beneficial effect of vitamin E supplementation on the biochemical and kinetic properties of Tamm–Horsfall glycoprotein in hypertensive and hyperoxaluric patients. Nephrol Dial Transplant. 2005; 20:1407–1415. [PubMed: 15855216]

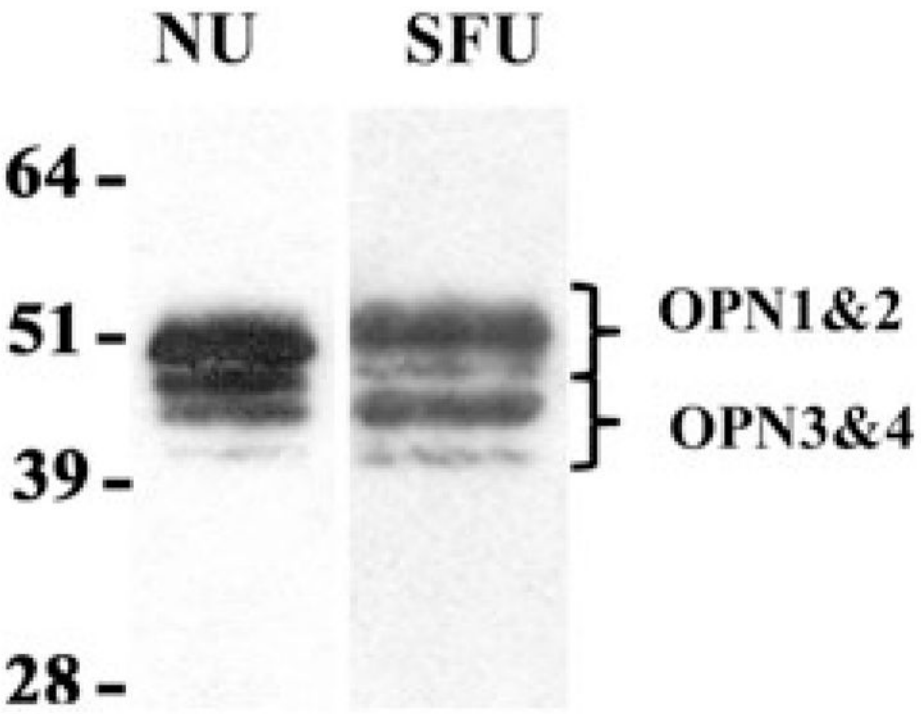

Fig. 1.
Human OPN detection in a standard Western blot from both NU and SFU

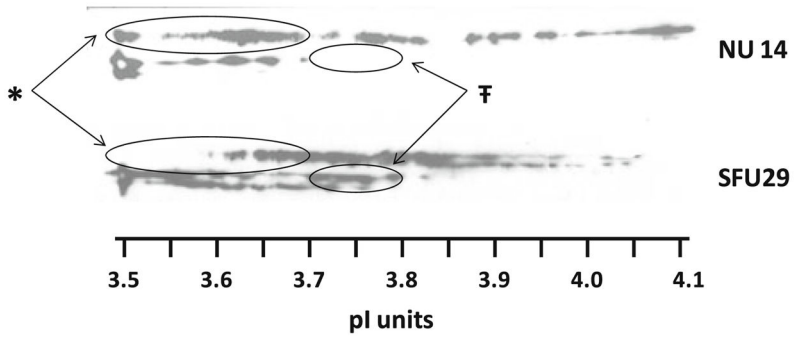

Fig. 2.

2D human OPN Western detection of representative NU and SFU samples run on 3.5–4.5 pI IEF strips. No signal was evident greater than a pI of 4.2. *Greater proportion of OPN 1 and 2 signal in the 3.5–3.7 range for NU versus SFU; 45 versus 10%, $P = 0.03$ (highlighted in the *large ovals*). Ŧ Lesser proportion of OPN 3 and 4 signal in the 3.7–3.8 range for NU versus SFU; 10 versus 18%, $P = 0.05$ (highlighted with the *small ovals*)

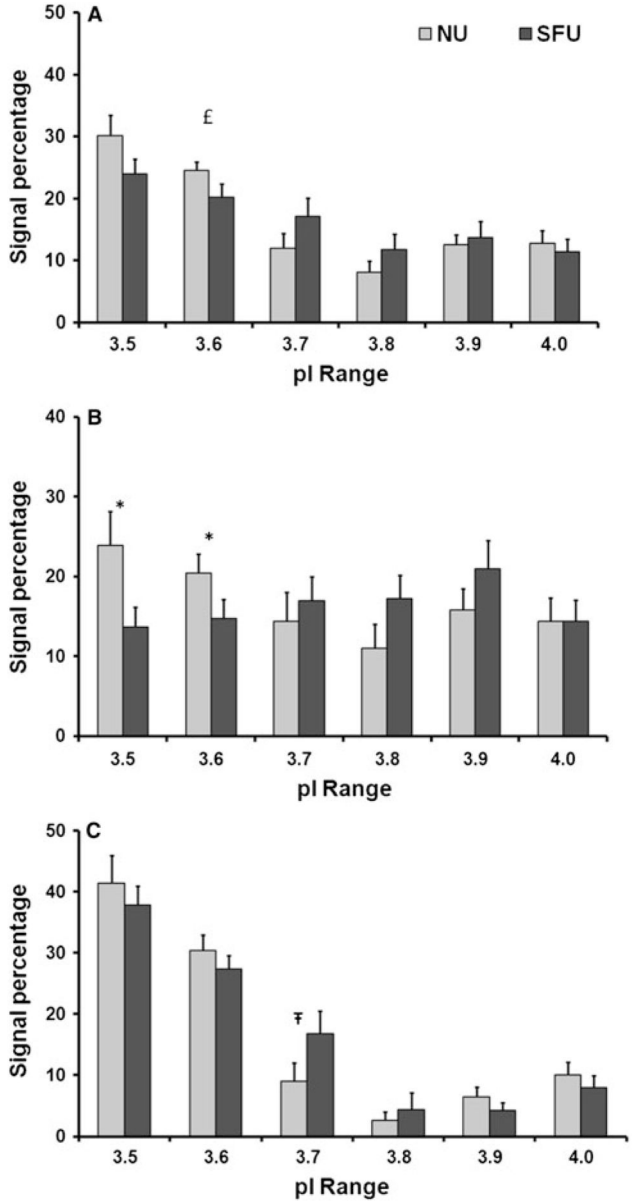

Fig. 3.

Bar graphs depicting the average percent signal per 0.1 pI increment for total OPN, OPN 1 and 2, and OPN 3 and 4. Total OPN signal (*panel A*) is significantly lower in SFU versus NU for the 3.6 region (£ = 0.04). The combined OPN 1 and 2 signal (*panel B*) is significantly lower in SFU versus NU for the 3.5 and 3.6 regions (* = 0.03). The combined OPN 3 and 4 signal (*panel C*) is significantly higher in SFU versus NU for the 3.7 region (₸=0.05). Standard *error bars* are shown

Table 1

Patient demographics

	Age	*n*	Male	Ca/Cr (mg/g)	Protein/Cr (mg/g)	# of stones	pH	Spec. grav.
NU	49 ± 10	13	11	100 ± 30	80 ± 30	None	5.7 ± 0.5	1.025 ± 0.007
SFU	46 ± 15	13	10	180 ± 70	110 ± 50	3 ± 2	6.2 ± 0.9	1.018 ± 0.009
P values	0.578			0.001	0.048		0.11	0.04

Table 2

Osteopontin concentrations based on ELISA

C-ELISA	OPN (μg/ml)	OPN (μg/mg creatinine)
NU	4 ± 2	2.6 ± 1.5
SFU	2.5 ± 1.5	3 ± 2
P values	0.23	0.38

Table 3

2D osteopontin Western blot analysis

Weight-averaged pI	NU (*n* = 13)	SFU (*n* = 13)	*P* values
All OPN	3.75 ± 0.03	3.77 ± 0.03	0.078
OPN 1 and 2	3.77 ± 0.04	3.81 ± 0.03	0.012
OPN 3 and 4	3.73 ± 0.04	3.73 ± 0.03	0.848

Table 4

Alkaline phosphatase-treated NU

Weight-averaged pI	NU untreated	NU treated	*P* values
All OPN	3.76 ± 0.02	3.80 ± 0.02	0.004
OPN 1 and 2	3.77 ± 0.03	3.82 ± 0.03	0.014
OPN 3 and 4	3.75 ± 0.01	3.78 ± 0.02	0.112